

Modelling the mechanical behaviour of concrete and other quasi-brittle materials

Reijo Kouhia

Tampere University, Structural Mechanics

March 24, 2026

Structural mechanics - current research topics

- Materials modelling
 - ▶ **Brittle or quasi-brittle materials: rock, concrete**, ice
 - ▶ Ductile materials: metals, polymers
 - ▶ Wood
- Fatigue modelling
- Coupled problems: magneto-electro-thermo-mechanics, thermo-hydro-chemo-mechanics
- Stability analysis, multibody mechanics

Sulata Dhakal
Juha Hartikainen
Reijo Kouhia
Jari Mäkinen
Timo Saksala
Jani Vilppo

Simulation of advanced rock drilling techniques

Timo Saksala

Collaboration with Mikko Hokka (TAU)

- Cracking enhanced using heat and/or high-voltage (HV), high-frequency (HF) electric shocks.
- Advanced FE method with embedded discontinuity field.
- Time-scales of heat transfer, mechanical response and electric field highly different.

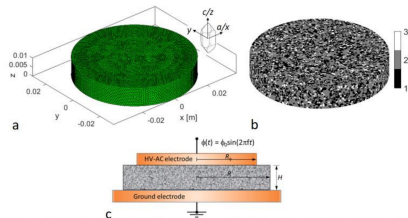


Fig. 4. Finite element mesh with 233066 tetrahedrons (a), rock mineral mesostructure (1=Quartz, 2=Feldspar, 3=Biotite) (b), and principle of HV-HF-AC actuation of rock sample (c).

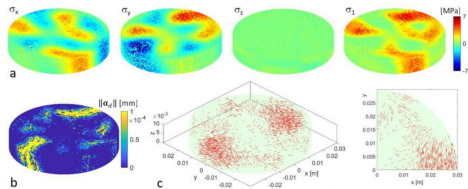


Fig. 7. Simulation results for AC piezoelectric actuation (Ref case with $\phi_0 = 25$ kV, $f = 125$ kHz): Stress component fields at the crest of 61st cycle (a), crack opening magnitude (b), and crack normal orientations (with every 20th crack plotted) (c) at the end of simulation.

Analysis of pretreatment of rock prior to comminution

- Comminution is an energy intensive process, pretreatment saves energy.
- Two kinds of pretreatment explored: heat shock and microwave heating.
- Advantage of heat shock: very high temperatures can be reached on the surface of rock in a short time.
- Advantage of microwave heating: selective heating of minerals (some absorbent and some transparent)

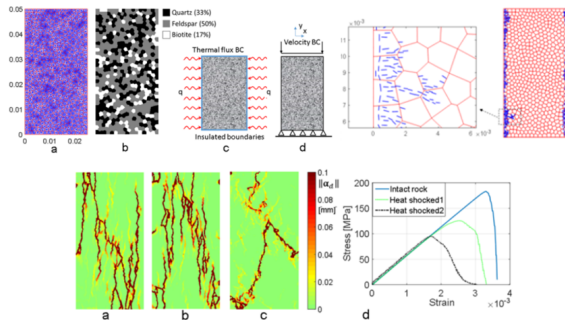
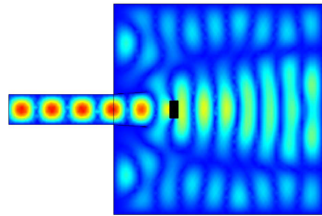
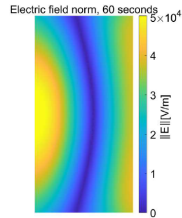


Figure 3. Simulation results for compression tests: final failures mode for intact rock a), heat shocked, cooled down case b), heat shocked and immediate compression c), average stress-strain curves for the three cases d).

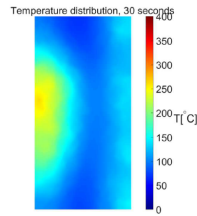
Microwave heating pretreatment



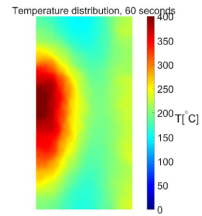
(a)



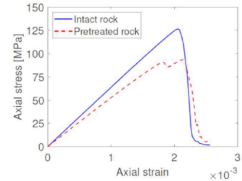
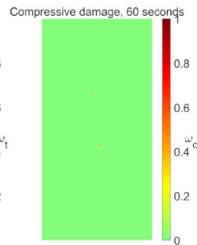
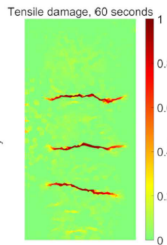
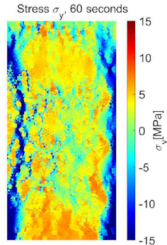
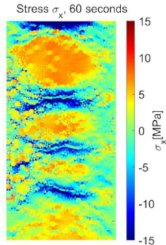
(b)



(a)

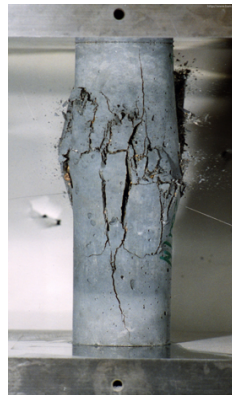


(b)



On concrete's mechanical behaviour

- The non-linear behaviour of quasi-brittle materials, like concrete and rock under loading is mainly due to damage and micro-cracking rather than plastic deformation.
- Damage of quasi-brittle materials can be modelled using scalar, vector or higher order damage tensors.
- Failure in tension is mainly due to the growth of the most critical micro-crack.
- Failure in compression can be seen as a cooperative action of a distributed microcrack array.



<http://mps-il.com>

Towards Sustainable Carbon Free Concrete Construction (ConSus)

Project funded the the Research Council of Finland, 1.9.2023-31.8.2026.

Participants:

- Oulu University (Srujana Gouda, Patrick Lemougna Ninla, Juho Yliniemi)
- VTT Technical Research Centre of Finland Ltd. (Kim Calonius, Alexis Fedoroff, Kari Kolari)
- Tampere University, (SD, JH, TS, RK)

Goal: To develop low CO₂ binders with strength and ductility comparable (or better) than Portland cement (PC) and computational methodology to analyse the behaviour of different concrete types.

About AAM mix design

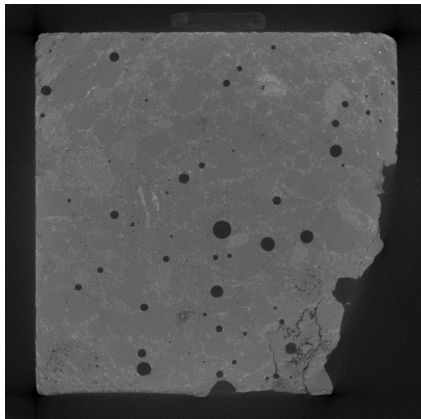
For years, Portland cement (PC) has been partly replaced by industrial waste such as blast furnace slag (BFS) to reduce CO₂ emissions.

Iron and steel making industry generate more than 400 million tonnes of slags worldwide

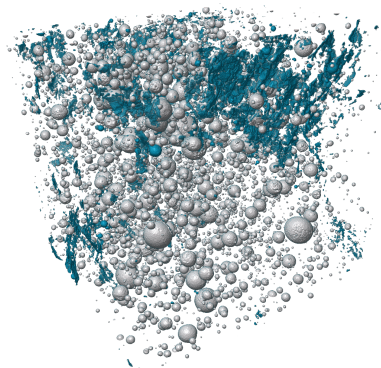
Blast furnace is going to be replaced by electric arc furnace (EAF).

Alkali-Activated Materials (AAM), also called geopolymers, has been found to be a promising alternative for PC. AAMs are consisting of precursor and alkali-activator: Commonly used precursors are for example fly ash, slag, and metakaolin, and alkali-activators are sodium silicate and sodium hydroxide.

Experiments - identifying damage due to loading (Alexis Fedoroff, VTT)

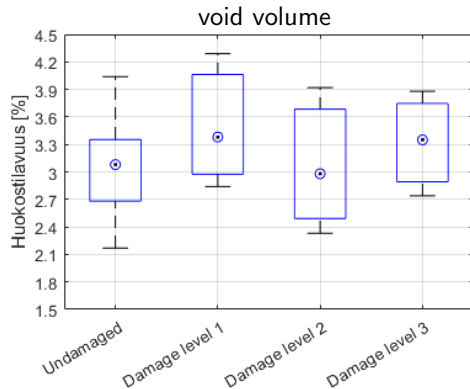
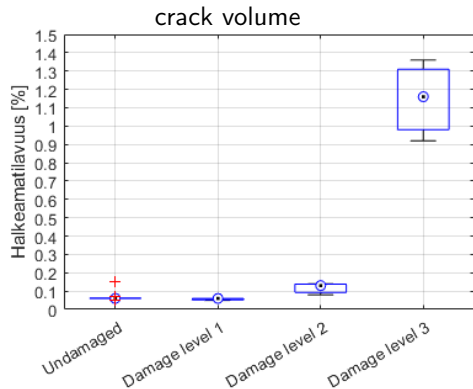


XCT scan of damaged specimen. Uniaxial compression at max. load.



3D model of crack (blue) and void (grey) distribution.

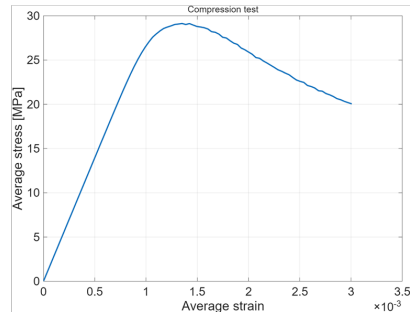
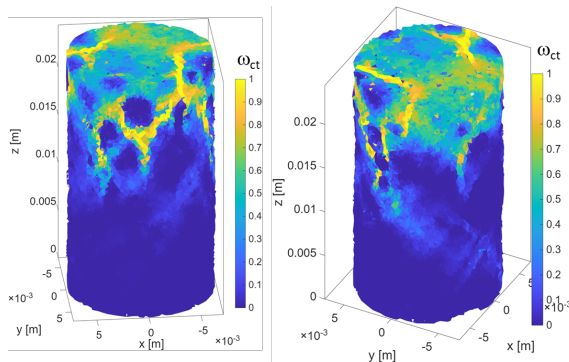
Identifying damage due to loading (cont'd)



level 1 $\approx 40\%$ of σ_c , level 2 at σ_c , level 3 in post peak region $\varepsilon \approx 1.2\varepsilon(\sigma_c)$.

Mesoscopic model, uniaxial compression

Two phase material, aggregate + cement paste, consistency viscoplastic DP two-surface model with Rankine tension cut-off for both phases. Isotropic damage with separate tensile and compressive components. 400 000 linear tetrahedra.



$$\omega_{ct} = 1 - (1 - \omega_c)(1 - \omega_t)$$

Macroscopic models

Our approach for macroscale model is to use CDM to imitate

Ottosen's Failure function

$$A \frac{J_2}{\sigma_c} + \Lambda \sqrt{J_2} + BI_1 - \sigma_c = 0$$

$$\Lambda = \begin{cases} k_1 \cos\left[\frac{1}{3} \arccos(k_2 \cos 3\theta)\right] & \text{if } \cos 3\theta \geq 0 \\ k_1 \cos\left[\frac{1}{3} \pi - \frac{1}{3} \arccos(-k_2 \cos 3\theta)\right] & \text{if } \cos 3\theta \leq 0 \end{cases}$$

$$\cos 3\theta = \frac{3\sqrt{3}}{2} \frac{J_3}{J_2^{3/2}}$$

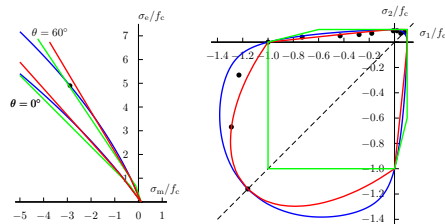
σ_c : the uniaxial compressive strength

$I_1 = \text{tr} \boldsymbol{\sigma}$: the first invariant of the stress tensor

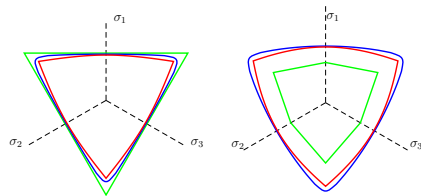
$J_2 = \frac{1}{2} \boldsymbol{s} : \boldsymbol{s}$, $J_3 = \det \boldsymbol{s} = \frac{1}{3} \text{tr} \boldsymbol{s}^3$: deviatoric invariants

A, B, k_1, k_2 : material constants

Meridian plane & plane stress



Deviatoric plane



π - plane

$\sigma_m = -f_c$

Green line = Mohr-Coulomb with tension cut-off

Blue line = Ottosen's model

Red line = Barcelona model, Lubliner et al.

Thermodynamic formulation

Two potential functions

$$\psi^c = \psi^c(S), \quad S = (\boldsymbol{\sigma}, \mathbf{D}, \kappa)$$

Specific Gibbs free energy

$$\gamma = \rho_0 \dot{\psi}^c - \dot{\boldsymbol{\sigma}} : \boldsymbol{\varepsilon}, \quad \gamma \geq 0$$

Clausius-Duhem inequality

$$\varphi(W; S), \quad W = (\mathbf{Y}, K)$$

Dissipation potential

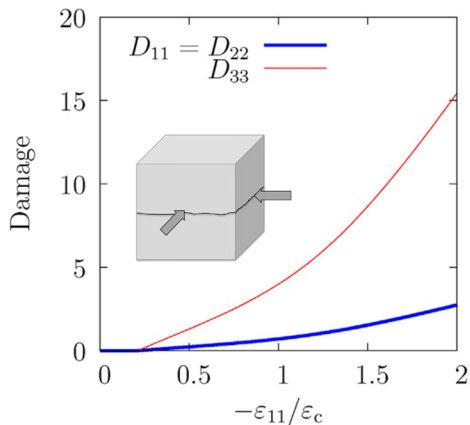
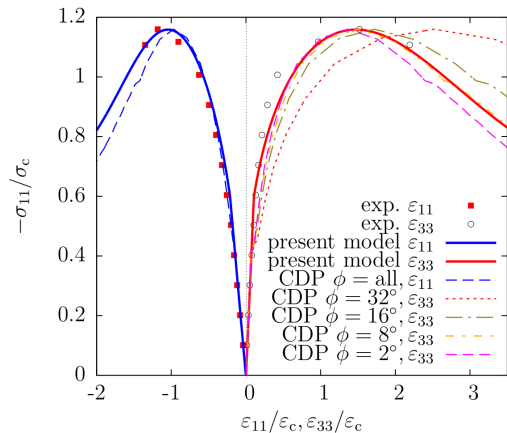
$$\gamma \equiv \mathbf{B}_Y : \mathbf{Y} + B_K K$$

$$\text{Define } \mathbf{Y} = \rho_0 \frac{\partial \psi^c}{\partial \mathbf{D}}, \quad K = -\rho_0 \frac{\partial \psi^c}{\partial \kappa}$$

$$\left(\rho_0 \frac{\partial \psi^c}{\partial \boldsymbol{\sigma}} - \boldsymbol{\varepsilon} \right) : \dot{\boldsymbol{\sigma}} + \left(\dot{\mathbf{D}} - \mathbf{B}_Y \right) : \mathbf{Y} + (-\dot{\kappa} - B_K) K = 0 \quad \forall \text{ admissible } \dot{\boldsymbol{\sigma}}, \mathbf{Y}, K$$

$$\Rightarrow \boldsymbol{\varepsilon} = \rho_0 \frac{\partial \psi^c}{\partial \boldsymbol{\sigma}}, \quad \dot{\mathbf{D}} = \mathbf{B}_Y, \quad \dot{\kappa} = -B_K$$

Equibiaxial compression test



(lhs) Stress-strain behaviour in equibiaxial compression ($\sigma_{11} = \sigma_{22}$) with experimental results from Kupfer et al. 1969. The Abaqus CDP model responses are shown for four values of the dilatation angle. Notice that different dilatation angle gives the best fit to experimental data in comparison to unconfined uniaxial compression for the CDP model.

(rhs) Damage-strain behaviour, damage is the largest in the 33-direction, i.e. the fracture mode corresponds splitting along the compressive plane illustrated.

Conclusions and future work

- Experimental data closer to computation.
- Better tools for coarsening/upscaling.
- International collaboration for open data needed.
- What are the most efficient numerical methods for materials fracturing simulations?
- Are ML, DL, EML, etc. GOOD, BAD or OGLY?

Thank You!